High-Speed Visible Imaging of the Central-Cell Plasmas in the GAMMA 10 Tandem Mirror

Yousuke NAKASHIMA, Nobuhiro NISHINO[1)], Yuta HIGASHIZONO, Hirokazu KAWANO, Shinji KOBAYASHI[2)], Mamoru SHOJI[3)], Yuusuke KUBOTA, Takayuki KOBAYASHI, Masayuki YOSHIKAWA, Hiroyuki HIGAKI, Md. Khairu ISLAM, Yoshiyuki MISHIMA and Teruji CHO

Plasma Research Center, University of Tsukuba, Tsukuba, Ibaraki 305-8577, Japan
[1)]*Graduate school of Engineering, Hiroshima University, Hiroshima 739-8527, Japan*
[2)]*Institute of Advanced Energy, Kyoto University, Gokasho, Uji 611-0011, Japan*
[3)]*National Institute for Fusion Science, Toki, Gifu 509-5292, Japan*

(Received 7 December 2006 / Accepted 26 April 2007)

Details of two-dimensional imaging performed in the central-cell of the GAMMA 10 tandem mirror by using high-speed camera are described. At the GAMMA 10 central-cell midplane, a high-speed camera (MEMRECAM fx-K4, NAC Inc.) was mounted and the shape and the motion of plasmas were precisely investigated. In the standard ion cyclotron range of frequency (ICRF) heated plasmas, gas puffing of hydrogen with short pulse (3-5 ms) close to the central-cell midplane was carried out to illuminate the periphery plasma and the time evolution of visible light emitted from the gas was captured. The Hα line-emission was localized close to the port of gas puffer. In the pellet injection experiments, 2-D images of the ablation light induced by hydrogen ice-pellet injection were successfully captured at the GAMMA 10 central-cell. Analysis of 2-D images clarified that the electron cyclotron heating applied in the central-cell (c-ECH) has a significant influence on the edge plasma turbulence and the ablation of hydrogen ice-pellet.

Keywords: GAMMA 10, tandem mirror, high-speed camera, two-dimensional image, plasma turbulence, gas puff imaging, pellet injection

DOI: 10.1585/pfr.2.S1056

1. Introduction

Two-dimensional (2-D) plasma diagnostics with high-speed cameras provides useful information on the edge plasma behavior. The gas puff imaging (GPI) technique with high-speed camera is a powerful method for visualizing the behavior of edge plasmas in 2-D images of visible light emission. In particular, recent development of the performance in high-speed cameras enables us to understand dynamics and detailed behavior of high temperature plasmas in many tokamak devices [1–3]. In the GAMMA 10 tandem mirror, edge plasma and neutral particle behavior have been investigated by measuring visible light and Hα line-emission together with neutral transport simulation using the DEGAS Monte-Carlo code [4] in order to evaluate the hydrogen recycling and particle balance in the tandem mirror plasmas [5–8]. In GAMMA 10, 2-D visible image measurements by using two high-speed cameras were started recently based on bi-directional collaboration between Hiroshima and Tsukuba Universities [9]. This collaborative experiments using GPI diagnostic technique clarified the detailed motion of plasma in the GAMMA 10 for the first time. In the latest collaborative work, pellet injection was performed in the central-cell and 2-D images of the ablation light induced by hydrogen ice-pellet injection are also successfully captured. In this paper, the results of 2-D imaging obtained with the high-speed camera are precisely presented in GPI and pellet injection experiments and the detailed behavior of periphery plasmas and neutrals is studied in terms of plasma-wall and pellet-plasma interactions.

author's e-mail: nakashma@prc.tsukuba.ac.jp

2. The GAMMA 10 Device and the Experimental Setup

2.1 GAMMA 10

GAMMA10 is a minimum-B anchored tandem mirror with thermal barrier at both end-mirrors [10, 11]. The device consists of an axisymmetric central-mirror cell, anchor-cells with minimum-B configuration produced by baseball coils, and plug/barrier cells with axisymmetric mirrors. In GAMMA 10 plasma is initialized by two plasma guns from both ends and then the main plasma is built up with two ion cyclotron range of frequency (ICRF) waves excited in the central-cell and anchor-cells, respectively. Recently, in order to increase the electron temperature in the central-cell, fundamental electron-cyclotron-heating (ECH) has been started by using a gyrotron microwave generator with 28 GHz and 400 kW. The locations of the west and east sides from the central-cell midplane are defined as positive values and as negative ones, respectively. A fixed limiters is installed in the central-cell near the central-cell midplane ($z = +30$ cm) with a diameter of 36 cm in order to limit the plasma diameter.

2.2 High-speed camera system

Figure 1 shows the cross-section of the GAMMA 10 central-cell and the location of high-speed camera. Hydrogen gas was puffed into the central-cell chamber from the bottom port near the midplane ($z = +12$ cm). Plasma was observed with a high-speed camera (fx-K4, NAC Inc.) from the horizontal view port in the south side (left side in Fig. 1). This camera is capable of capturing 2-D images of 160×80 pixels in 60000 frames per second, which is suitable in the experimental condition of GAMMA 10. In this experiment, a measuring parameters of 192×144 pixels in 40000 frames per second is also used. A photograph of the interior of the central vacuum chamber viewing from the midplane port is shown at the bottom of Fig. 1. The central limiter and the exit of the gas puffer are located and the visible emission from gas puffing and ablation light from the ice-pellet can also be observed through the port. Captured 2-D image data are transferred to a PC via optical fiber data-link and monitored by another PC in the control room using the remote-desktop system.

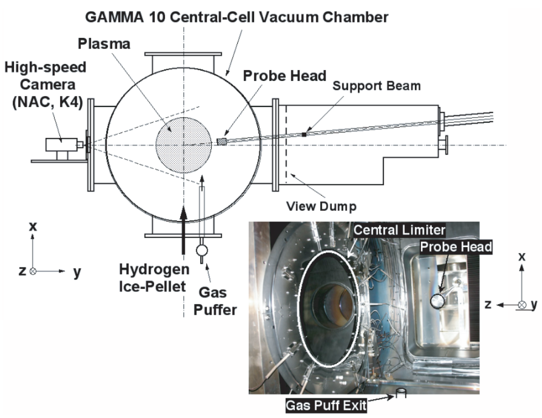

Fig. 1 Cross-section view of the GAMMA 10 central-cell and viewing area of the high-speed camera. Photograph of the interior of the central-cell vacuum chamber.

3. Experimental Results and Discussion

3.1 Gas puff imaging experiment

Figure 2 shows an example of the time behavior of plasma parameters in the GPI experiment carried out in

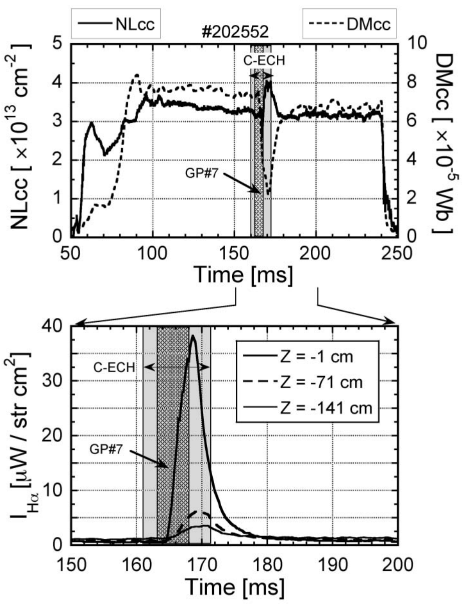

Fig. 2 Time behavior of plasma parameters in GPI experiment. (a) electron line-density and diamagnetism in the central-cell, (b) Hα line intensity signal.

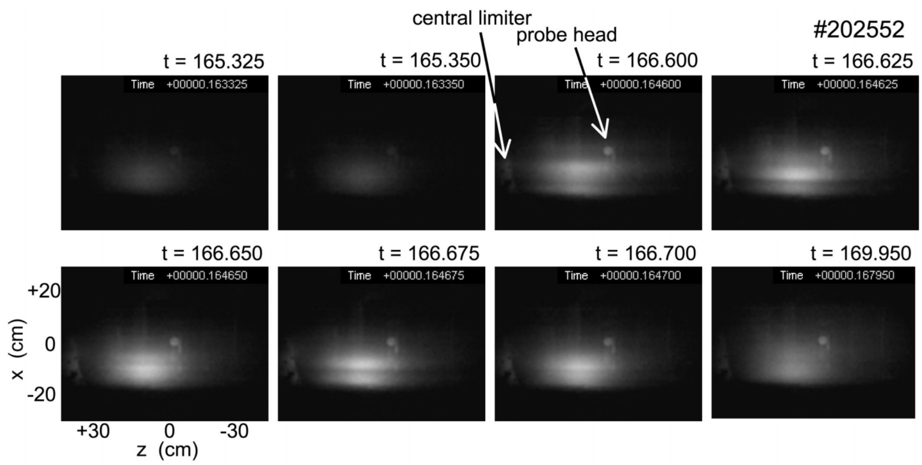

Fig. 3 Time evolution of 2-dimensional visible images during gas puff imaging experiment.

standard hot ion mode plasmas of GAMMA 10. The plasma is produced by ICRF from 50 ms to 240 ms and GPI is performed in the period of potential confinement by using plug ECH (160.5-170.5 ms). The gas puffing is carried out from the bottom of the central-cell midplane (GP#7) in the period of 163-168 ms. As shown in Fig. 2 (a), the increase of line density by 20 % and considerable decrease of the diamagnetism caused by the gas puffing are observed, which imply the excess of puffing gas to some extent. During the gas puffing, it is found that Hα line intensity at the midplane ($z = -1$ cm) increases by a few tens times higher than that before the gas puffing. On the other hand, the Hα intensity 70 cm away from the midplane is smaller by 1/7 times with respect to that of at $z = -1$ cm, which clearly indicates the localization of hydrogen gas around the exit of gas puffer.

In Fig. 3, the detailed time evolution of measured 2-D images during the gas puffing (t = 165.3 ms to 172 ms) is shown at an interval of 0.25 ms. In this shot, a wide band interference filter including Hα wavelength (λ = 650 nm, $\Delta\lambda_{\mathrm{FWHM}} \sim$ 80 nm) is placed in front of the high-speed camera lens so that the filter may permeate the Hα light entering at a wide-angle. In this range of wavelength it is confirmed that there are no major spectra without Hα emission, which shows that the images mainly due to the Hα line emission. In an initial period of the gas puff (t = 165.325-165.350 ms), a clear localization of visible emission cloud induced by the gas puffing from the bottom port is observed in front of the exit of the gas puffer. As shown in the figure, in the period of illumination (166.6-166.7 ms), a filament-like structure along the line of magnetic force and its motion are revealed in the plasma column. It has been found that this motion is anti-clockwise to the direction of the magnetic field line with the frequency range of 5-8 kHz. After the gas puffing is terminated ($t \geq$ 169.95 ms), such structure and motion fades away. On the other hand, experiments without C-ECH show that such activities of the plasma turbulence during GPI are significantly small, which indicates that the application of C-ECH may enhance the turbulence in this experimental condition.

3.2 Pellet injection experiment

The time evolution of the plasma parameters measured during a pellet injection in the hot ion mode plasma is shown in Fig. 4. The line density of the central-cell plasma

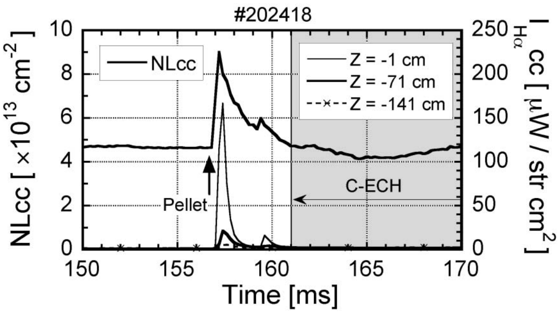

Fig. 4 Time behavior of electron line-density and Hα line intensity in the pellet injection experiment.

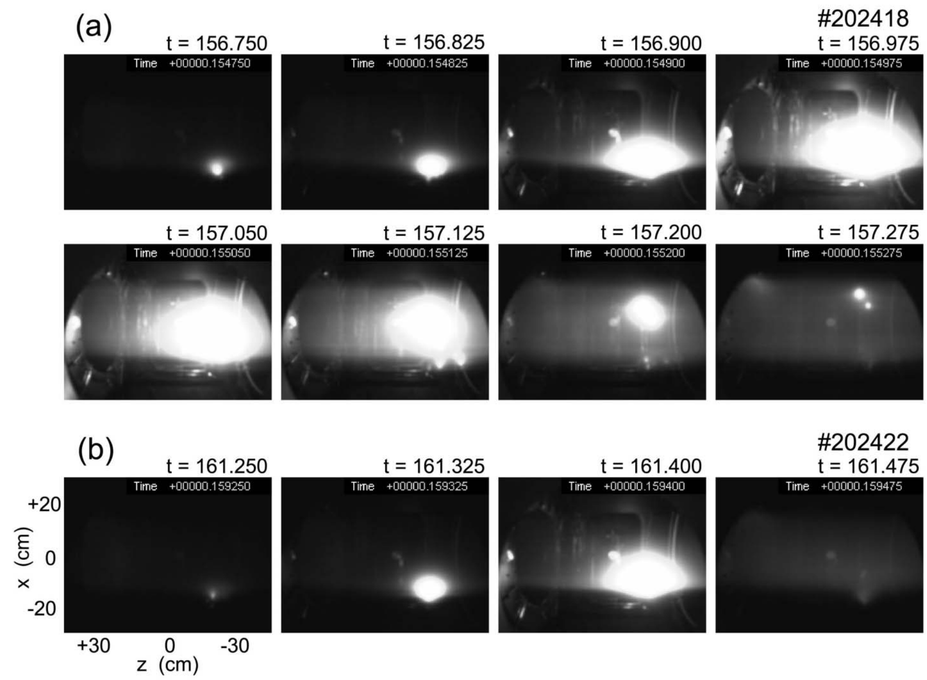

Fig. 5 Detailed 2-dimensional visible images during pellet injection experiment, (a) in the case without C-ECH, (b) in the case with C-ECH.

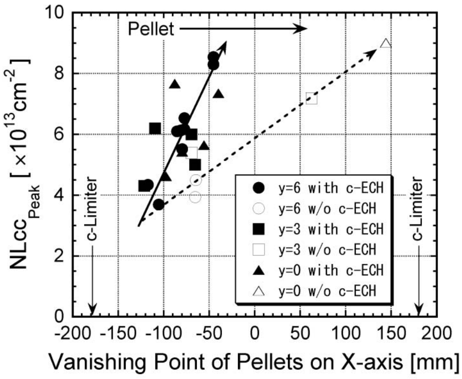

Fig. 6 Correlation between the penetration length of pellets and achieved plasma line-density.

is observed to attain up to $9 \times 10^{13}\,\mathrm{cm}^{-2}$ due to the pellet injection. Hα intensity measured near the injection port ($z = -12$ cm) increases by more than 100 times compared to the base intensity. Under the same condition, an experiment in which the timing of C-ECH is close to that of pellet injection is conducted.

Figure 5 shows the time evolution of 2-D visible images captured at the pellet injection experiment shown in Fig. 4. In these two shots, the pellet is broken into several fragments in the course of transportation in the guide tube and these images are focused on one piece. In Fig. 5 (a), each 2-D image is shown from the start of ablation light (156.75 ms) to the time of fading out (157.275 ms) at intervals of 3 frames (0.75 ms). The pellet is injected before the C-ECH pulse (161-201 ms) and no power from C-ECH contributes the pellet ablation in this shot. As shown in the figure, the ablation light traverses the plasma and vanishes near the upper edge of the plasma. This indicates that the pellet passed through the plasma column. It is also confirmed that the ablation light expands along the magnetic field line.

In contrast to the above result, the ablation light with C-ECH disappears in the course of passing the plasma column as shown in Fig. 5 (b). In the case of C-ECH, electrons are strongly heated and it is recognized that the electron temperature significantly increased. Accordingly it is considered that the enhancement of ablation due to the increase of electron temperature prevents the penetration of the pellet.

In Fig. 6, the peak values of attained line density are plotted as a function of vanishing point of the pellets on x-axis. In the pellet injection experiments, the density measurement using microwave interferometer is carried out in 3-different position (y = 0, 3 and 6 cm). Data are plotted as a parameter of its position in y-axis. From the figure, it is found that no pellets can penetrate far beyond the plasma center in the case with C-ECH. In each y-position of the interferometer, there is a noticeable tendency that the deeper penetration of pellets attains the higher line density. In the case with C-ECH, almost the same line density is achieved in the shorter penetration length. The above results predict that the higher plasma density can be achieved by fueling up to the deeper region with large pellets and C-ECH.

4. Summary

Two-dimensional imaging was performed in the central-cell of the GAMMA 10 tandem mirror by using high-speed camera. The Hα-line emission was localized close to the port of the gas puffer. The filament structure observed in GPI has rotative motion of the frequency 5-8 kHz and is strongly revealed with C-ECH. In the pellet injection experiments, 2-D images of the ablation light induced by hydrogen ice-pellet injection were also successfully captured at the GAMMA 10 central-cell. A strong correlation between the penetration length of the pellet and the attained plasma density is recognized and the effect of C-ECH is also confirmed. These results show clearly the usefulness of 2-D image analyses for guiding principles in high-density tandem mirror experiments.

Acknowledgement

This study was supported by the bidirectional collaboration research program in the University of Tsukuba, Hiroshima University, Kyoto University and NIFS. The authors would like to acknowledge the members of the GAMMA 10 group, University of Tsukuba for their help in the experiments.

[1] S.J. Zweben *et al.*, Phys. Plasmas **9**, 1981 (2002).
[2] R.J. Maqueda *et al.*, Rev. Sci. Instrum. **74**, 2020 (2003).
[3] J.L. Terry *et al.*, J. Nucl. Mater. **290-293**, 757 (2001).
[4] D. Heifetz, D. Post, M. Petravic *et al.*, J. Comput. Phys. **46**, 309 (1982).
[5] H. Higaki *et al.*, Rev. Sci. Instrum. **75**, No.10 Part II, 4085 (2004).
[6] Y Nakashima *et al.*, J. Nucl. Mater. **196-198**, 493 (1992).
[7] Y. Nakashima *et al.*, J. Nucl. Mater. **241-243**, 1011 (1997).
[8] Y. Nakashima *et al.*, J. Plasma Fusion Res. SEREIS **6**, 546 (2004).
[9] N. Nishino, Y. Nakashima *et al.*, Plasma and Fusion Res. **1**, 035 (2006).
[10] M. Inutake *et al.*, Phys. Rev. Lett. **55**, 939 (1985).
[11] T. Cho *et al.*, Trans. Fusion Technol. **47**, No.1T, 9 (2005).